

Temperature dependence of glass-transition cooperativity from heat-capacity spectroscopy: Two post-Adam-Gibbs variants

H. Huth, M. Beiner, and E. Donth

Fachbereich Physik, Universität Halle, D-06099 Halle (Saale), Germany

(Received 21 July 1999)

The Adam-Gibbs paper [G. Adam and J. H. Gibbs, *J. Chem. Phys.* **43**, 139 (1965)], one of the most cited works in physics, has a continuing influence on research into glass transition. This paper is generally considered as the turning point from rare free volume to small configurational entropy as the reason for slow molecular mobility in glass formers. The reader, however, is confronted with a dilemma. The slowing down is conceptually linked with increasing cooperativity, but in fact we find only a formula for a link of mobility with configurational entropy. Neither the size of cooperativity nor its temperature dependence can be calculated from Adam-Gibbs formulas. The present paper compares predicted temperature dependences of cooperativity for two post Adam-Gibbs variants — the first via the configurational entropy and the second via a fluctuation approach — with the temperature dependence of cooperativities determined by means of heat-capacity spectroscopy (HCS) data for polystyrene, polyisobutylene, and a random copolymer (SBR 1500). The data yield a strong increase of cooperativity with lower temperature and, taking previous HCS data into account, indicate a cooperativity onset about 100 K above the Vogel temperature for these polymers. An acceptable fit of the cooperativity data can formally be reached by both post Adam-Gibbs variants only upon the condition that this onset is included. The problem of a final decision between both variants and the conceptual differences between the configurational entropy approach and the fluctuation approach to glass transition are discussed.

I. INTRODUCTION

The main conclusion of the Adam-Gibbs (AG) paper¹ was that “The molecular-kinetic theory proposed in the present paper explains the temperature dependence of relaxation phenomena in glass-forming liquids essentially in terms of the temperature dependence of the size of the cooperatively rearranging region” (CRR). AG “define a cooperatively rearranging region as a subsystem of the sample which, upon a sufficient fluctuation in energy (or, more correctly, enthalpy), can rearrange into another configuration independently of its environment.” In other words, CRR’s are defined by statistical independence of their thermal fluctuations with relation to glass transition. The formulas obtained are [AG Eq. (10)]

$$S_c = N s_c \quad (1.1)$$

with S_c being the extensive configurational entropy of a macroscopic supersystem composed of N subsystems (=CRR’s), and s_c is the extensive configurational entropy of the subsystem of z monomeric units. Further, [AG Eq. (20)] they introduce a critical size of a CRR for transition events marked by an asterisk (*):

$$z^* = N_A s_c^* / S_c, \quad (1.2)$$

where S_c is now the *molar* configurational entropy of the macroscopic sample and N_A is the Avogadro constant. The main result is [AG Eq. (21)]

$$\bar{W}(T) = \bar{A} \exp(-\Delta\mu s_c^* / kT S_c) = \bar{A} \exp(-C/TS_c), \quad (1.3)$$

where C is a constant, k is the Boltzmann constant, $\bar{W}(T) \sim 1/\tau(T)$ is the transition probability that is reciprocally re-

lated to the relaxation time $\tau(T)$, and $\Delta\mu$ is “largely the potential energy hindering the cooperative rearrangement per monomer segment.” This is an interpretation in the sense of Simon² that structural relaxation is not associated with a collective barrier, i.e., in the sense of Goldstein’s subsequent energy landscape.³ AG suggested that the dependence of $\Delta\mu$ on T and z can be neglected. As seen from Eq. (1.3), s_c^* is then also considered as a constant. AG stressed that the derivation of Eq. (1.3) “is based essentially on the assumption of independent and equivalent subsystems,” i.e., CRR’s. We see, however, that $z(T)$, in other words the number of particles in a CRR, cannot be calculated from Eqs. (1.2) and (1.3) (nor from other AG formulas), since S_c in Eq. (1.1), when related to one mole, is trivial with respect to N and s_c . This situation will be called the “AG dilemma.”

There are essentially two approaches to escape from the dilemma. These phenomenological approaches will be called “post AG variants” in this paper:

First variant = S_c variant. The first variant tries to find a reformulation without leaving the configurational entropy concept. Matsuoka⁴ scales the temperature dependence of s_c^* with respect to S_c . He assumes that $s_c^* \rightarrow 0$ for $T \rightarrow 0$ but, of course, $S_c \rightarrow 0$ for $T \rightarrow T_0$, where T_0 is the Kauzmann or Vogel temperature. This gives

$$z \sim T/(T - T_0). \quad (1.4)$$

Matsuo *et al.*,⁵ “assuming that the entropy within the CRR is zero,” calculate the CRR size from

$$z(T) = s_c^* N_A / S_c(T), \quad (1.5)$$

where $s_c^* = \text{const}$ is for a single molecule, and S_c is for one mole. They extrapolate their precise experimental $S_c(T)$ data to high temperatures and find then

$$S_c(T) = s_c^* N_A - C'/T^2, \quad (1.6)$$

where C' is a constant obtained from the extrapolation. Both methods give a moderate increase of CRR size for lower temperatures. They obtain values between 4 and 10 molecules or monomeric units at the glass temperature $T = T_g$,

$$z(T_g) = 4 - 10. \quad (1.7)$$

In a more general argumentation: starting from the Kauzmann extrapolation⁶

$$S_c(T) \sim T - T_0, \quad T > T_0 \text{ but near } T_0, \quad (1.8)$$

and assuming that the cooperativity has something to do with $S_c(T)$ we expect from the AG equation, Eq. (1.3),

$$z(T) \sim 1/(T - T_0), \quad T > T_0 \text{ but near } T_0. \quad (1.9)$$

This expectation is reflected by the Matsuoka formula Eq. (1.4), whereas the Kauzmann temperature T_0 is not directly reflected in the Matsuo formula Eq. (1.6).

Second variant = fluctuation variant. The CRR size is calculated using a Nyquist-type fluctuation formula.⁷ This approach corresponds directly to the AG CRR definition by statistical independence of relevant thermal fluctuations. Calling z now N_α , $z \equiv N_\alpha$, we get the cooperativity from

$$N_\alpha = RT^2 \Delta(1/c_V) / M_0 \delta T^2, \quad (1.10)$$

where $\Delta(1/c_V) = (1/c_V)^{\text{glass}} - (1/c_V)^{\text{liquid}}$ with c_V being the isochoric specific heat capacity, and δT the temperature fluctuation of one average CRR which can be calculated from the transformation interval at T_g (Ref. 8) or from the dispersion of the imaginary part of dynamic heat capacity, C_p'' , as determined by means of heat-capacity spectroscopy (HCS).⁹⁻¹¹ The isochoric specific heat will be approximated⁸ by the isobaric specific heat, $\Delta(1/c_V) \approx \Delta(1/c_p)$.

General problems with temperature fluctuation of subsystems will be discussed in a parallel paper.¹² This paper contains a comparison of the statistical J. W. Gibbs approach (no temperature fluctuation) with the thermodynamic von Laue¹³ approach (with temperature fluctuation). Eq. (1.10) is based on the latter. The paper¹² contains also a proposal how a combination of dynamic neutron scattering, specific-heat capacity, and dielectric compliance can be used to decide the temperature-fluctuation issue by experiments in the crossover region.

The temperature dependence obtained^{7,14} by using a fluctuation relation to the Williams-Landel-Ferry¹⁵ (WLF) equation for $\tau(T)$ is stronger than Eq. (1.4),

$$N_\alpha \sim (T - T_0)^{-2}. \quad (1.11)$$

The CRR sizes at T_g are in fact larger⁷ than those from the first variant, Eq. (1.7),

$$N_\alpha(T_g) = 35 - 290. \quad (1.12)$$

A first independent and quantitative determination from exchange NMR methods for spin diffusion¹⁶ obtained a characteristic length of $\xi_\alpha = 3 \pm 1$ nm for CRR's in polyvinylac-

etate, in accordance to that from the fluctuation approach. This length corresponds to N_α of order 100 particles per CRR (Ref. 17) and does not correspond to the estimations based on the S_c variant [Eq. (1.7)].

The sensitivity of calorimetric cooperativity to confinement of glass formers in pores¹⁸ and between layers¹⁹ of larger dimension (5–12 nm) indicates that the condition of statistical independence for the CRR definition is sensitive to small disturbances induced by such a confinement.

Recent HCS results show directly an onset of the cooperative α relaxation in the crossover region^{9,10} as previously indicated by dielectric measurements.²⁰⁻²² For the cooperativity close to the α onset we observed, so far, for five substances^{10,11}

$$N_\alpha(T) \sim (T_{\text{onset}} - T)^2, \quad T < T_{\text{onset}}. \quad (1.13)$$

This result is confirmed by differential scanning calorimetry (DSC) along a homologous series of polymers whose onset temperature systematically approaches T_g .²³ Interpolating between Eqs. (1.11) and (1.13) we obtained¹¹ for the fluctuation variant

$$N_\alpha^{1/2}(x) = A \frac{1-x}{x}, \quad 0 < x < 1, \quad (1.14)$$

and by analogy, from Eqs. (1.9) and (1.13) for the S_c variant

$$N_\alpha^{1/2}(x) = A' \frac{1-x}{\sqrt{x}}, \quad 0 < x < 1, \quad (1.15)$$

where A and A' are constants, and x is a reduced temperature,

$$x = (T - T_0) / (T_{\text{onset}} - T_0), \quad (1.16)$$

where $x=0$ for the Kauzmann or Vogel temperature T_0 and $x=1$ for the onset temperature T_{onset} .

The crossover is hardly indicated by the temperature dependence of configurational entropy defined as $S_c = S_{\text{melt}} - S_{\text{crystal}}$. Only a weak bend is occasionally observed in the melt heat capacity.²⁴ The AG relation Eq. (1.3), however, breaks down above the crossover.²⁵ Viscosity and dielectric relaxation time change their temperature dependence above the crossover.²⁶⁻²⁹ Since the material is frozen for $T < T_g$ our analysis is altogether restricted to $T_g < T < T_{\text{onset}}$.

The general aim of the present paper is to look for a criterion that can decide between the two post AG variants. The methodical problem is that at present such a decision must be based on cooperativities experimentally determined by means of the fluctuation variant, since the S_c variant does not give an independent way to experimental determination of cooperativities. The *ad hoc* use of configurational entropy for determination of cooperativity in the first variant is not suited for its test. On the other hand, Eq. (1.10) of the fluctuation variant allows a determination of cooperativity as a function of temperature by HCS independently from any *ad hoc* assumption about this temperature dependence. The only open point³⁰ of Eq. (1.10) is if subsystem temperature can in fact fluctuate.¹² Our idea is, therefore, to determine $N_\alpha(T)$ from experimental HCS data using the fluctuation formula [Eq. (1.10)] and to compare the results with the temperature dependences as obtained for the two post AG variants [Eqs.

TABLE I. Characteristic properties [T_g = glass temperature; M_w and M_0 = molecular weights of polymer chain and monomeric unit, respectively; $m = d(\log \omega)/d(T_g/T)|_{T=T_g}$ = fragility (Ref. 33)]; of the polymers.

Sample	T_g (K)	M_w (kg mol ⁻¹)	M_0 (g mol ⁻¹)	m
SBR 1500 ^a	215	≈ 500	61	97
PIB	201	101	56	43
PS	373	270	104	117

^aSBR 1500 is a random styrene butadiene copolymer containing 23w% styrene and is not crosslinked.

(1.14) and (1.15)]. The experimental problem is whether the experimental $N_\alpha(T)$ values from HCS are precise enough or not to discriminate between the different temperature dependences. The general problem is to formulate the conceptual differences between the two post-Adam-Gibbs variants for understanding glass transition, briefly: cooperativity vs configurational entropy.

II. EXPERIMENTAL RESULTS FROM HEAT-CAPACITY SPECTROSCOPY (HCS)

Heat-capacity spectroscopy (HCS = 3ω method^{31,32}) was used to get the calorimetric parameters of Eq. (1.10) for three amorphous polymers, polystyrene (PS), polyisobutylene (PIB), and a random styrene butadiene copolymer (SBR 1500), in the frequency range from 0.02 to 2000 Hz. Some properties of the polymers are given in Table I. To enlarge the quality of the data at least three temperature runs on at least two different nickel heaters were performed for each sample. Small nickel heaters (about 1.5×6 mm²) were used for high frequencies (>1 Hz), while larger heaters (about 5×10 mm²) were used for low frequencies (0.02–20 Hz). This ensures that the signal amplitude and precision is large enough at high frequencies (amplitude $\sim \omega^{-1/2}$), while the thermal wavelength is small compared to the heater dimension at low frequencies, as required by the data evaluation concept.^{34,35} Further experimental details of our HCS setup and data evaluation method are described elsewhere.^{36,37}

Typical isochronous ($\omega = \text{const}$) effusivity data, $\rho\kappa_p^*(\omega, T) = \rho\kappa_p'(\omega, T) - i\rho\kappa_p''(\omega, T)$, as obtained from our HCS setup are shown in Fig. 1. An upwards step in the real part and a corresponding peak in the imaginary part, as typical for compliances at the dynamic glass transition, were obtained for all samples and frequencies. Transferring the different peak maxima in an Arrhenius plot ($\log \omega$ versus $1/T$), we obtained WLF (Ref. 15) shaped traces (Fig. 2). The calorimetric traces for PS and SBR1500 are parallel to the corresponding dielectric traces. Only a small frequency shift (<0.3 decades) between both traces is observed, similar as for other polymers.³⁸ The large (about one decade) frequency gap between HCS and dielectric traces in polyisobutylene is probably due to a second relaxation process at frequencies slightly above the α transition. This was previously observed by shear measurements in a wide frequency-time range.^{39,38}

In order to calculate the cooperativity from our HCS data [Eq. (1.10)] we have to extract the pure dynamic heat capacity, $c_p^*(\omega, T)$, from our HCS effusivity data, $\rho\kappa_p^*(\omega, T)$. We extract $c_p^*(\omega, T)$ data by calibrating the HCS data with

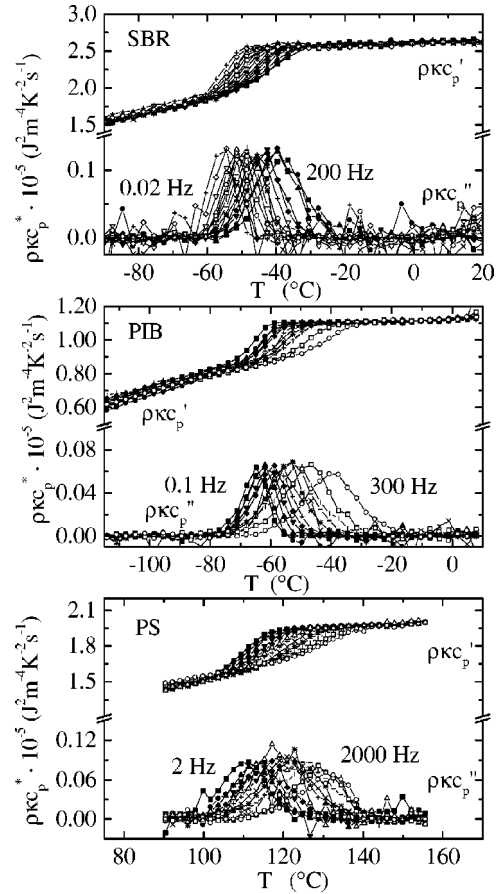


FIG. 1. Real and imaginary parts of dynamic effusivity, $\rho\kappa_p^* = \rho\kappa_p' - i\rho\kappa_p''$, from heat-capacity spectroscopy (HCS) for SBR 1500 rubber, polyisobutylene (PIB), and polystyrene (PS) as function of temperature.

DSC and temperature modulated dynamic scanning calorimetry data (TMDSC). Two assumptions are necessary for this procedure: (i) frequency independence of $\rho\kappa$, and (ii) temperature independence of $\rho\kappa$. The first assumption (i) is widely accepted. There are different experimental tests^{40–42} that $\rho\kappa$ is practically frequency independent in the range of the dynamic glass transition. The remaining uncertainty of this approximation seems to be smaller than 10% in the HCS frequency window. More critical is the second assumption (ii). Serious information about the temperature dependence of thermal conductivity for polymers are rare. Moreover, the $\kappa(T)$ data in the literature are partly less defined. Usually, the temperature dependence is small, of order 10%/100 K, and, if any, a slight bend near T_g is indicated. To test the $\rho\kappa(T) = \text{const}$ assumption for our polymers we divided the low-frequency HCS data by $c_p(T, \omega)$ data from TMDSC at a comparable frequency. This temperature dependence of $\rho\kappa$ is of the order a few percent for SBR 1500, PIB, and PS in the HCS temperature range (Fig. 3). The calculation of $\Delta(1/c_p)$ would only be influenced if the $\kappa(T)$ function change in the HCS dispersion zone is so large that the tangent construction (see below) used to determine $\Delta(1/c_p)$ would fail. This is obviously not the case (Fig. 3). The peak width, δT , would be influenced if the peak shape is significantly modified by the underlying changes in $\kappa(T)$. This can be excluded because the relevant temperature interval, $2\delta T$

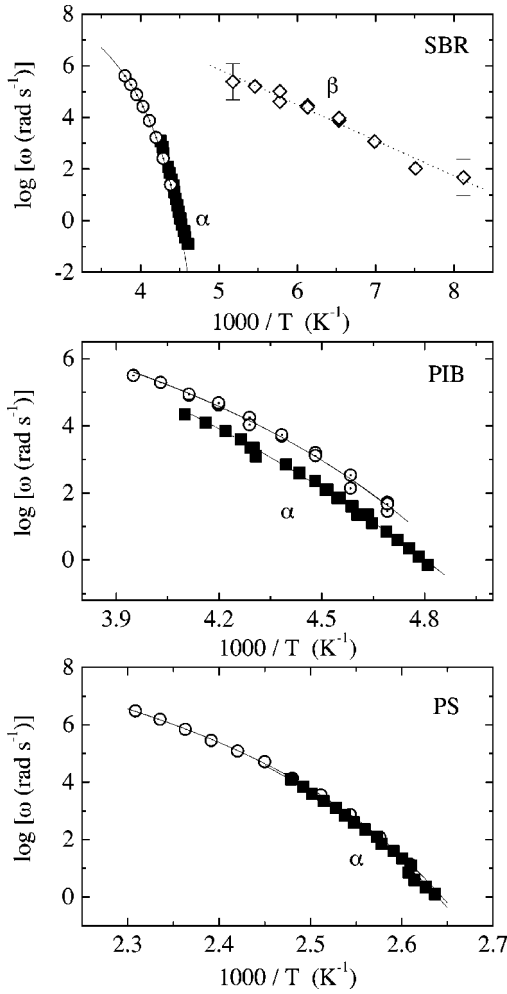


FIG. 2. The α peak frequencies from HCS (■) and dielectric spectroscopy (○), on \log_{10} scale, versus inverse temperature for SBR 1500, PIB, and PS. The solid lines are fits to the data with the WLF equation $\log \omega = \log \Omega - B/(T - T_0)(T_0 = \text{Vogel temperature, } \log \Omega = \text{logarithm of the asymptotic frequency, } B = \text{curvature})$. Dielectric data for the β process (◇) in SBR 1500 are added. The dotted line corresponds to an Arrhenius temperature dependence.

<20 K, is too small for a significant change of $\kappa(T)$. In summary, we think that the influence of a residual $\rho\kappa(\omega, T)$ function on our calorimetric parameters, $\Delta(1/c_p)$ and δT^2 , can be neglected because its variation in the relevant temperature region is small.

The data reduction procedure in Fig. 3 allows us also to check the precision of our absolute $\rho\kappa c_p^*$ values. The calculated $\rho\kappa$ values are compared to literature data for $\rho\kappa$ in Table II. The data are in agreement if the large absolute HCS uncertainty is taken into account. A comparison of $\rho\kappa$ data from different HCS runs on one and the same sample (Table II) indicates the value of this absolute uncertainty. The consistency of data at different frequencies for one temperature run on one heater is better because the main uncertainty comes from effects of different heater and sample dimensions.³⁶ The data from different runs were, as mentioned above, finally normalized by TMDSC calibration to get comparable values for $\Delta(1/c_p)$ in gK/J. The corresponding $\rho\kappa$ prefactors are listed in the first column of Table II. The shape of the $\Delta(1/c_p)(T)$ curves is not affected by this fixed-factor normalization.

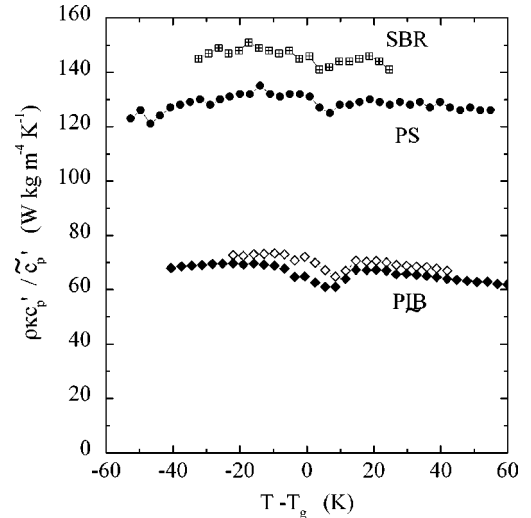


FIG. 3. Calibration ratio $\rho\kappa c_p' / \tilde{c}_p'$ versus temperature for SBR 1500 (□), PIB (◇) and PS (●). Dynamic effusivity $\rho\kappa c_p'(T)$ is from HCS at 0.02 Hz (SBR 1500, PS) or 0.1 Hz (PIB). Dynamic heat capacity \tilde{c}_p' is from temperature-modulated DSC (Ref. 67) at (1/60)Hz. The ratio $\rho\kappa c_p' / \tilde{c}_p'$ for PIB (◇) with \tilde{c}_p' from conventional DSC ($dT/dt = -10$ K/min) is additionally given. Note that the particularity for PIB near T_g results probably from the frequency shift between HCS and TMDSC (or DSC).

Figure 4 demonstrates how the calorimetric parameters, δT and $\Delta(1/c_p)$, were determined from normalized HSC data: The $\Delta(1/c_p) = (1/c_p)^{\text{glass}} - (1/c_p)^{\text{liquid}}$ values were taken by a tangent construction to the $c_p'(T)$ data from the real part isochrones ($\omega = \text{const}$), while the δT values were obtained from a fit with the Gauss function to the imaginary part of $c_p^*(T) = c_p'(T) - i c_p''(T)$. Note that the statistical error of the parameters obtained and the uncertainty of the $\rho\kappa$ normalization procedure influence only the absolute N_α values, not the general shape of the $N_\alpha(T)$ curves. In the sense of Eqs. (1.14) and (1.15) only the prefactors A and A' are affected, not the functional dependence of N_α on reduced temperature. The uncertainty of absolute N_α values from DSC and TMDSC is estimated in Ref. 8.

The calorimetric parameters, δT and $\Delta(1/c_p)$, for our three polymers have a well defined temperature dependence [Figs. 5(a) and 5(b)]: The δT value increases linearly with T , while the $\Delta(1/c_p)$ values decrease systematically. The onset temperatures T_{onset} were estimated by a linear extrapolation of $\Delta c_p(T)$ to zero, the Vogel temperatures T_0 were taken from a WLF fit of dielectric data. The dielectric T_0 values are comparable but more precise than the Vogel temperatures taken from a WLF fit of our HCS data. The onset temperature T_{onset} is comparable with the temperature T_β , where the dynamic glass transition α and the Johari Goldstein process β (Ref. 43) merge in the crossover region of SBR 1500 ($T_\beta \approx 295 - 325$ K) and PS ($T_\beta \approx 425$ K).⁴⁴ Typical uncertainties for the T_0 and T_{onset} values in Table III are about ± 10 K.

An extrapolation to high temperature gives $\delta T(x=1) \approx 15$ K at the onset, in good agreement with the experimental value $\delta T \approx 20$ K at the onset of the α process directly measured in poly(*n*-hexyl methacrylate).⁹ A linear extrapolation of δT to low temperatures would give $\delta T = 0$ at a finite x

TABLE II. Density and thermal conductivity near the glass temperature.

Sample	$\rho\kappa$ (kg W m ⁻⁴ K ⁻¹) from HCS	$\rho\kappa$ (kg W m ⁻⁴ K ⁻¹) from literature
SBR 1500	147 (1st run)	177–233 ($T=25$ °C) ^a (Ref. 62)
	141 (2nd run)	202–204 ($T=20$ °C) (Ref. 63)
	136 (3rd run)	
PIB	67 (1st run)	103–109 ($T=20$ °C) ^b (Ref. 64)
	68 (2nd run)	120 ($T=20$ °C) (Ref. 63)
	75 (3rd run)	118 ($T=T_g$) (Ref. 65)
		119 ($T=25$ °C) ^b (Refs. 62 and 66)
PS	125 (1st run)	131 ($T=T_g$) (Ref. 63)
	159 (2nd run)	131–161 ($T=T_g$) (Ref. 66)
	136 (3rd run)	134 ($T=T_g$) (Ref. 62)
		168–174 ($T=T_g$) (Ref. 65)

^aCrosslinked SBR 1500 rubber.

^bIsobutylene isoprene rubber = vulcanized isobutylene isoprene copolymer containing <3 mol% isoprene.

>0 for all samples. This may be an indication for an exhaustion^{30,45} of the possibilities of free volume to drive the glass transition before the Vogel temperature could be reached. Actually, we have no physical argument for a linear extrapolation to lower temperatures. The relaxation strength, $\Delta(1/c_p)$, as a function of temperature is individually curved [Fig. 5(b)].

The isothermal frequency dispersion $\delta \ln \omega$ [Fig. 5(c)] was estimated by the local temperature time equivalence

$$\delta \ln \omega = \delta T \cdot (d \ln \omega / dT)_{\text{WLF}}, \quad (2.1)$$

where the derivative was calculated along the calorimetric trace in a $\log \omega$ - T plot. For SBR 1500 the dielectric WLF parameters were used. The calorimetric Kohlrausch exponent (Table III) was calculated from

$$\beta_{\text{KWW}} \approx 1.07 / \delta \ln \omega. \quad (2.2)$$

The main experimental result of this paper, the temperature dependence of cooperativity N_α , is presented in two different ways: versus reduced temperature x in Fig. 5(d) and directly versus temperature in Fig. 6. The square root of co-

operativity $N_\alpha^{1/2}$ is a curved function of temperature T for all three polymers. It increases dramatically for low temperatures (small x) and tends to vanish near the onset temperature T_{onset} ($x=1$). The lines in Fig. 6 are fits with the two post-Adam-Gibbs variants, the configuration-entropy variant [Eq. (1.15), dashed lines] and the fluctuation variant [Eq. (1.14), solid lines]. The thin lines are for the original equations [Eqs. (1.9) and (1.11)] without consideration of the crossover. These curves do not correspond to the experimental data. The bold lines, including the onset correction, approximate the data much better. This means that the existence of a cooperativity onset is indicated even by the cooperativity data far below the crossover. The fitted onset temperatures T_{onset} (Table III) are similar to the values as observed from the $\Delta c_p(T) \rightarrow 0$ extrapolation described above. The difference is about 10–20 K, with the higher T_{onset} values from the $\Delta c_p \rightarrow 0$ extrapolation. The differences are larger for the configuration entropy variant than for the fluctuation variant, but always smaller than 20 K. The experimental uncertainty of the linear $\Delta c_p(T) \rightarrow 0$ extrapolation is comparable.

The mean deviations χ^2 from the fits with both post-Adam-Gibbs variants are comparable (Table III). This means that our HCS data cannot discriminate between them. The $N_\alpha^{1/2}(x)$ or $N_\alpha^{1/2}(T)$ data are more curved than expected (see deviation plots of Fig. 6).

The parameters A of Eq. (1.14) vary between 6.4 and 10.3 (Table III), i.e., A is not a universal but an individual constant. This was also observed in Ref. 11. The $N_\alpha^{1/2}(x)$ data for different polymers, therefore, do not collapse in a single curve [Fig. 5(d)]. Fitting formally the data by $N_\alpha \sim (T - T_0)^{-y}$ would yield $y = 5 \pm 1$ in the available temperature range for the investigated polymers (see Table III). The product $\delta \ln \omega \cdot \delta T$ increases systematically with reduced temperature x for the three investigated polymers [Fig. 5(e)].

Figure 5 demonstrates the difficulty to discriminate between the two post AG variants including the onset behavior.

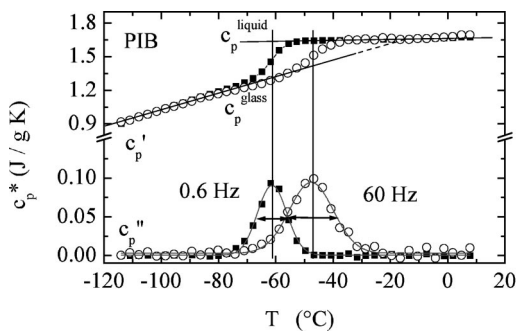


FIG. 4. Example for the construction used for determination of calorimetric parameters, δT (Gauss fit, the double arrows are $2\delta T$) and $\Delta(1/c_p) = (1/c_p)^{\text{glass}} - (1/c_p)^{\text{liquid}}$ [tangents in liquid and glass zone of the $c_p'(T)$ curves], from normalized HCS data.

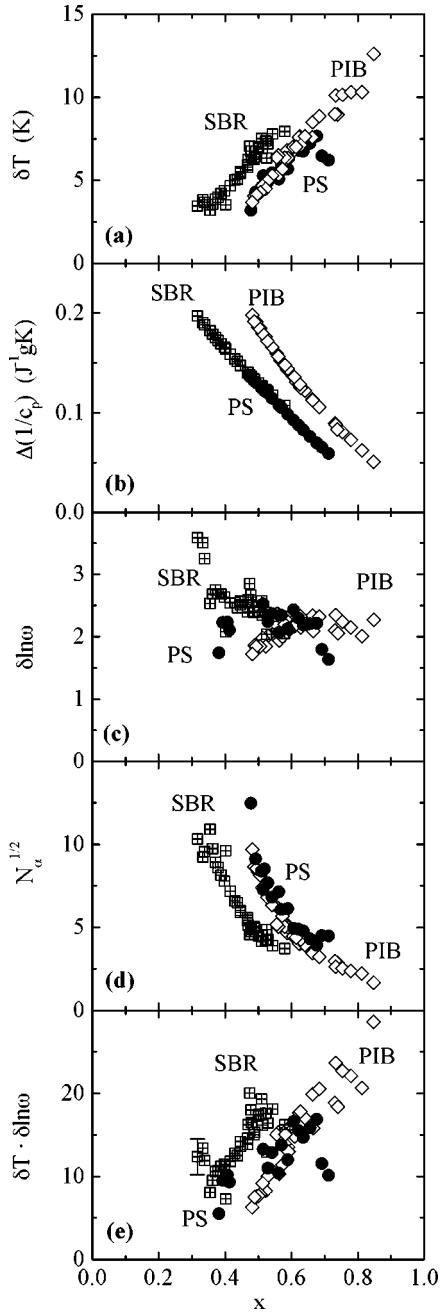


FIG. 5. Calorimetric parameters for the determination of cooperativity, δT (a) and $\Delta(1/c_p)$ (b), estimated frequency dispersion $\delta \ln \omega$ (c), square root of cooperativity $N_\alpha^{1/2}$ (d), and the product $\delta T \cdot \delta \ln \omega$ (Ref. 46) (e) as function of reduced temperature $x = (T - T_0)/(T_{\text{onset}} - T_0)$ for SBR 1500, PIB, and PS.

Informative x values smaller than 0.3–0.5 (depending on fragility) are not possible because of freezing at T_g . Informative x values larger than 0.6–0.8 (depending on the A value) need not be helpful because the behavior is there dominated by the onset behavior. After choosing substances with a large informative x interval we can only enlarge the data precision and the frequency range of HCS to get data suited for a decision between the variants.

Another way to decide between the two post-AG variants may be the use of absolute experimental^{8,16} cooperativities at T_g [$N_\alpha(T_g) \approx 100$]. To get such large cooperativities from the S_c approach, with its small variation range from Eq. (1.6), would imply to connect the high-temperature critical s_c^* values not with a single particle, $z^* = 1$,⁴⁷ but with larger subsystems, $z^* > 1$, e.g., $z^* \approx 10$ (cf., e.g., Ref. 48). HCS data for the a process at $T > T_{\text{onset}}$ show, however, $N_\alpha \approx 1$.^{9,49} The $z^* > 1$ proposal inside the S_c variant does not lead to an adequate explanation for the large cooperativities at T_g .

Our general idea to understand the small $N_\alpha \approx 1$ values for the a process is⁵⁰ to connect them with a cage, including the first coordination shell, as used in the interpretation of the a process beyond the crossover, $T > T_{\text{onset}}$, by mode coupling theory.⁵¹ We think that for $T > T_{\text{onset}}$ the molecular cooperativity is localized at the cage door for escaping of the “central” particle, whereas for $T < T_{\text{onset}}$ escaping requires the assistance of a cooperativity shell in the molecular environment of the cage. The details require a discussion of the N_α behavior across the crossover region⁵⁰ and a general interpretation³⁰ of the small N_α values of order 1, both outside the scope of this paper.

The temperature dependence of $N_\alpha(T)$ seems to ignore the real liquid structure. At low temperature, N_α is much larger than the first coordination number (of order 10), at high temperature N_α is significantly smaller than 10. At least for two substances, PIB (Fig. 5) and benzoin isobutylether,⁵² $N_\alpha(T)$ covers smoothly the $N_\alpha \approx 10$ region without particularity in the frame of the uncertainties. We expect that this is a general phenomenon and suggest calling it *disengagement* of dynamic heterogeneity from liquid structure.

From an experimental point of view, the fluctuation variant seems to be a real alternative to the S_c variant. The change of dynamics at the crossover is explicitly indicated by a definite change of cooperativity as calculated from the fluctuation formula Eq. (1.10). This change could not be expected from the smooth dependence of $S_c(T)$ or from the moderate bend of the landscape excitation profile there. In

TABLE III. Vogel temperatures and fit parameters for both post AG variants [Eqs. (1.14) and (1.15)].

Sample	T_0 (K)	$\Delta c_p \rightarrow 0$ T_{onset} (K)	S_c variant [Eq. (1.15)]			Fl variant [Eq. (1.14)]			y	β_{KWW} [Eq. (2.2)]
			A'	T_{onset}	χ^2	A	T_{onset}	χ^2		
SBR 1500	184	289	11.8	262	0.51	6.2	277	0.44	4.0	0.43 ± 0.05
PIB	159	259	11.5	252	0.96	7.7	258	0.65	5.6	0.49 ± 0.05
PS	330	433	15.4	419	0.88	9.8	427	0.78	4.9	0.49 ± 0.05

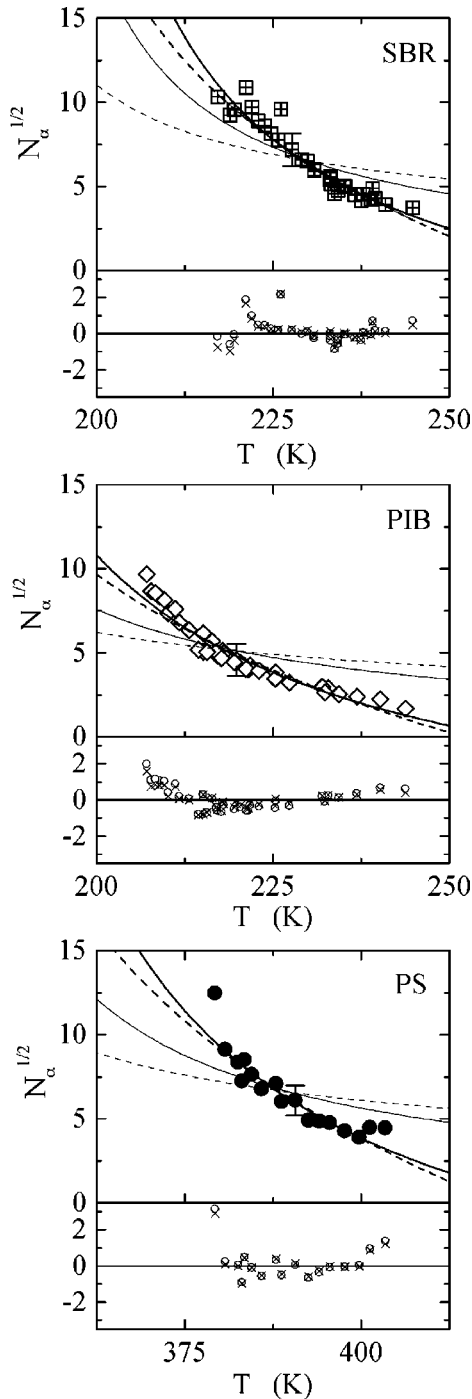


FIG. 6. Cooperativity as function of temperature for SBR 1500, PIB, and PS. The lines are fits to the data by the configuration-entropy variant (dashed lines) and the fluctuation variant (solid lines). Bold lines are obtained using Eqs. (1.14) and (1.15) with cooperativity onset, thin lines are from Eqs. (1.9) and (1.11) without cooperativity onset. Typical errors are indicated and are considered during the fitting procedure. The fit parameters are given in Table III. Deviation plots for the configuration-entropy variant [Eq. (1.14), \circ] and for the fluctuation variant [Eq. (1.15), \times] are given in the lower parts.

the next section we will therefore discuss some conceptual differences between the fluctuation approach and the conventional approaches to glass transition such as configurational entropy, landscape paradigm, and dynamic heterogeneity.⁵³

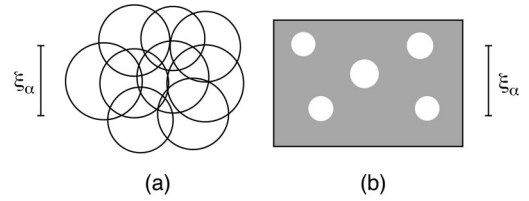


FIG. 7. Cooperatively rearranging regions (CRR's) for no dynamic heterogeneity (a) and for the Glarum defect diffusion realization of dynamic heterogeneity (b). White = islands of mobility, large $\log \omega$. Gray = cooperativity shells, low $\log \omega$. ξ_α = characteristic length = average size of a CRR. The low density contrast of the part (b) pattern makes it appear as shade upon molecular pictures.

III. CONCEPTUAL DIFFERENCES

A. Adam-Gibbs paper relationships

In the AG paper,¹ statistical independence was only used for additivity to make statistics with subsystems. To get the maximal term of an isothermal-isobaric configurational partition function, a Δ_c factor in Δ for $G = z\mu = -kT \ln \Delta$, they “sort the subsystems into two classes, those, n in number, that reside in states which allow a cooperative rearrangement and the $N - n$ that are in states not allowing a transition.” The result is

$$\Delta_c(z, p, T) = \sum_{E_{\text{pot}}, V} w_c(z, E_{\text{pot}}, V) \exp(-E_{\text{pot}}/kT) \times \exp(-pV/kT). \quad (3.1)$$

The configurational entropy S_c was then expressed directly as the logarithm of configurations W_c of the maximal term of the partition function. This procedure is reflected in a second, slightly varied definition of a CRR “as the smallest region that can undergo a transition to a new configuration without a requisite simultaneous configuration change outside its boundary.”¹

To get the explicit relationship of S_c and dynamics [Eq. (1.3)] they gauged the general relation at high temperature with critical CRR transition values for z and s_c , z^* for s_c^* . Since the cooperativity was only aimed to handle the additivity they did not try to obtain an explicit formula for $z(T)$.

B. Statistical and energetic independence

We consider two extreme variants of the subsystem independence problem with respect to dynamic heterogeneity.

(i) *No dynamic heterogeneity.* In this variant we think that, in principle, each molecule can be the center of a non-trivial CRR as defined by statistical independence [Fig. 7(a)]. The result is a large overlap of CRR's with no reflection of them neither in the Gibbs distribution nor in the energy landscape. The additivity needed for a thermodynamic analysis by subsystems is guaranteed by the Riesz representation theorem of probability theory.⁵⁴ Supposing that to each continuous function u vanishing outside a finite interval (outside any CRR) there corresponds a number $\mathbf{E}(u)$ with the following properties: linearity, i.e.,

$$\mathbf{E}(c_1 u_1 + c_2 u_2) = c_1 \mathbf{E}(u_1) + c_2 \mathbf{E}(u_2), \quad (3.2)$$

positivity [$u \geq 0$ implies $\mathbf{E}(u) \geq 0$], and normalizability. Then there exists a unique probability distribution F with

$$\mathbf{E}(u) = \int u(x)F\{dx\}. \quad (3.3)$$

Identifying $\mathbf{E}(u)$ with the internal energy, $dU = TdS - pdV$, Eq. (3.3) means to find always, irrespective of the overlap in Fig. 7(a), an additive set $\{dx\}$, i.e., a set of CRR subsystems which is representative for a thermodynamics of the whole sample.

To mitigate the shock of Fig. 7(a), we should remark that Eq. (1.10), from which our cooperativity was determined, stems only from temperature fluctuation. The conjugate variable in thermodynamics is not the energy or the enthalpy itself, but the entropy with no direct relation to energy pictures.

The statistical independence of Fig. 7(a) CRR's is decoupled from the energetic independence of Landau-type subsystems as mediated by the Gibbs distribution

$$\begin{aligned} E_{\text{pot}}(q_1, q_2) \\ &= E_{\text{pot}}(q_1) + E_{\text{pot}}(q_2) \Rightarrow \exp(-E_{\text{pot}}(q_1, q_2)/kT) dq \\ &= \exp(-E_{\text{pot}}(q_1)/kT) dq_1 \cdot \exp(-E_{\text{pot}}(q_2)/kT) dq_2. \end{aligned} \quad (3.4)$$

The intermolecular potentials are not switched-off for the overlap picture Fig. 7(a). The same must be assumed for small z^* of order one in the AG approach. Statistical independence directly derived from Eq. (3.4) would prevent large variation of cooperativity with temperature as well as small cooperativities inside the second configuration shell.

Note that the CRR's are functional, i.e., they are exclusively related to the Fourier components of the slow molecular movements with frequencies in the dispersion zone of the α process of dynamic glass transition. It is their part of the temperature fluctuation that is exclusively used in our Eq. (1.10) for N_α . This large and slow fluctuation (δT^2) cannot be quenched by thermal conductivity due to the fast phonons.

(ii) *With dynamic heterogeneity.* Let us now assume to have a dynamic heterogeneity⁵⁵ in the special form of a fluctuating spatiotemporal pattern of local α mobility, $\log \omega$. As a concrete model we think about a Glarum defect diffusion model,⁵⁶ interpreted as a cage whose escaping ability below the crossover is retained, as mentioned above, by means of an assisting cooperativity shell in the environment.⁵⁰ Each CRR consists then of a cage = an island of mobility⁵⁷ in a cell of lower mobility [Fig. 7(b)]. The average size of a CRR, ξ_α , is defined by the average distance between the islands.

Assume that (i) beside the Maxwell factor, only a potential intermolecular energy E_{pot} is needed for an explanation of the dynamic glass transition, and (ii) that the Gibbs distribution contains fluctuation enough for this purpose. Then⁶⁸ such a pattern must be reflected by the Gibbs distribution (being then the ‘‘static’’ boundary for this dynamic heterogeneity), by the structure, and by the landscape. We do not think, again, that the CRR independence is directly mediated by the range of intermolecular potentials as expressed in Eq.

(3.4). The question instead is how large is the contrast of the Fig. 7(b) pattern. We discuss the contrast problem in relation to the landscape paradigm.

The landscape paradigm⁵⁸ is a popular concept to discuss the glass transition dynamics in a one-dimensional picture with many molecular potential barriers. The hope is to get a better insight from this picture than from other one-dimensional (related to space) pictures as, e.g., from the intermediate structure function $S(Q, t)$ or its Fourier transforms. The problem is to get a precise map from the high-dimensional configuration space $\{q\}$ to the one-dimensional landscape, precisely enough to discuss details or even subtleties of slow dynamics.

Note the different dimensions d of related constructions. The energy hypersurface, $E_{\text{pot}}(q)$, should at least include the relevant subsystem, a CRR. Its dimension is $d = f_p N_\alpha$, where f_p is the number of degrees of freedom of what is counted as a particle. The real, geometrical space where structure and dynamics are measured has $d = 3$, of course, and the landscape is considered as a function of one ‘‘collective coordinate,’’ $d = 1$.

Let, for instance, a landscape basin be defined⁵⁹ by a partition of the configuration space such that a local minimization of $E_{\text{pot}}(q)$ maps any point in a basin to the same minimum. At lower temperature, i.e., with cooperativity, the sampling shifts to lower energies and mutual access among basins becomes subject to considerable activation, the system explores minima with substantially higher energy barriers. We may think about craters⁵⁸ in the landscape. Such a landscape is related to configurational entropy by an excitation profile.⁶⁰ Is this landscape picture really informative about our cooperativity?

In general, energetic separation implies statistical independence, but the inverse is not always true. There are examples for statistical independence in systems whose parts are strongly coupled by energy. An old example are playing cards: an ace of hearts couples physically the independent events of getting aces and hearts. In a way, the independence and functionality of CRR's corresponds to the play, not to the deck of cards. Since statistical independence can, in principle, be imagined without energetic barriers [Fig. 7(a)] it is not *a priori* agreed that a CRR must correspond to craters or something similar with high-energy barriers. Are there perhaps secret paths for the subsystem point in the high-dimensional $E_{\text{pot}}(q)$ hypersurface corresponding to cooperativity and avoiding the postulated barriers? Is cooperativity formed by competition of many equivalent pieces of a ‘‘collective’’ path in a ‘‘rugged’’ $E_{\text{pot}}(q)$ hypersurface yielding a ‘‘gentle’’ one-dimensional (1D) landscape for the α process? Especially if the density contrast corresponding to the 3D island picture for mobility $\log \omega$ [Fig. 7(b)] is small? Since the landscape is mainly determined by the steep intermolecular repulsion potentials it seems legitimate to consider density contrast instead of barrier heights.

The 3D density contrast of the Glarum pattern was estimated to be extremely weak at low temperatures. We used a free-volume treatment of Glarum defects by means of Levy limit distributions.^{30,45} From a partition of a CRR into partial systems, inside a CRR, we get a ‘‘fluctuating’’ free volume v_f of order $N_\alpha^{-1/\alpha}$, invariant against partition variants. This

free volume is related to one average CRR and will be used as a measure for the density contrast for cooperativity,

$$c^* = N_\alpha^{-1/\alpha}. \quad (3.5)$$

The power law follows directly from Levy scaling with the Levy exponent $\alpha = \beta_{\text{KWW}}$. The contrast c^* of Eq. (3.5) decreases dramatically when the cooperativity increases as for low temperatures below the crossover. Putting the contrast $c^* = 1$ at a crossover with $N_\alpha = 1$, we get a relative density contrast of order 10^{-4} for $N_\alpha = 100$ and $\alpha = 1/2$. *Large, independent CRR's need not be represented by high-energy barriers.* Such low contrast also does not allow us to conclude that a characteristic length is absent when structure research fails to find it. At present, structure experiments are sensitive to a contrast larger than 10^{-2} or 10^{-3} , say.

Note that the density contrast of Eq. (3.5) for cooperativity is much smaller than the density contrast due to thermal density fluctuations of CRR's monitored by the compressibility. The latter contrast is of order $c = N_\alpha^{-1/2}$, since the relevant Gauss distribution corresponds to a Levy exponent $\alpha = 2$. The cooperativity contrast c^* is a subtlety of the $E_{\text{pot}}(q)$ hypersurface that can appear in low dimensions only after careful averaging (as, e.g., realized by a scattering experiment on a large sample $\gg \xi_\alpha$). It seems extremely difficult to find a precise map from the high-dimensional configuration space to a one-dimensional landscape picture that can realize a real-space cooperativity contrast of order $c^* = 10^{-4}$.

Assume that the Vogel temperature T_0 is a measure of the landscape roughness⁶¹ in the temperature range of a specific²⁸ WLF equation. The Vogel temperature T_0 for the α process above the crossover is larger than T_0 for the α process below the crossover.²⁸ We expect from the small Vogel temperature that the landscape roughness below the crossover is in fact smaller than above the crossover. Large CRR's defined by statistical independence cannot easily be detected: We had to look for a tiny contrast in a nonrugged landscape.

C. Exhaustion effect

There are indications that at low temperatures the cooperativities become larger than even expected from the fluctuation variant (Fig. 5 and Ref. 11). Can cooperative dynamics

really be monitored by such small density contrasts as indicated by Eq. (3.5) for $N_\alpha > 100$? Two qualitative possibilities evolving from too small a contrast can be imagined. Either the cooperativity will become larger than indicated by $N_\alpha^{1/2} \sim 1/x$ for low temperatures because the Glarum defect cannot explore the whole cooperativity cell — the possibilities of the defect diffusion are “exhausted” — or the cooperativity will become smaller due to other processes (such as an α precursor between α and β process) that may help the liquid to remain mobile. The larger N_α values for the lower temperatures in Fig. 5 may indicate the first possibility. They correspond to small contrast $c^* < 10^{-3}$.

IV. CONCLUSION

The temperature dependence of molecular cooperativity observed by means of heat-capacity spectroscopy indicates a general behavior: A cooperativity onset in the crossover region and strong increase at low temperatures. Cooperativity seems an alternative concept that should be admitted for comparison with conventional concepts for explanation of dynamic glass transition, such as configurational entropy, landscape paradigm, and dynamic heterogeneity. Molecular cooperativity corresponds to the original strategy of Adam and Gibbs. The low contrast of cooperativity is a subtlety which causes that cooperativity can only be measured by extremely sensitive methods. We used statistical independence accessible by thermal fluctuations via the fluctuation-dissipation theorem. Possibly, the main mystery of glass transition — how can the individual, multifarious structures of different glass formers produce a general mobility pattern in the Arrhenius plot — may be understood by relating the different facets of glass transition to the cooperativity of the α process. The main advantage of cooperativity is to have an additional intuitive parameter: the characteristic length for the α process with a definite temperature dependence.

ACKNOWLEDGMENTS

We thank Dr. K. Schröter and Dr. S. Kahle for many discussions of the cooperativity issue, Dr. E. Hempel (Halle) and Professor C. Schick (Rostock) for providing the TMDSC curves, the Deutsche Forschungsgemeinschaft DFG (Sonderforschungsbereich SFB 418), and the Fonds Chemische Industrie FCI for financial support.

¹G. Adam and J. H. Gibbs, *J. Chem. Phys.* **43**, 139 (1965).

²F. Simon, *Ergeb. Exakten. Naturwiss.* **9**, 222 (1930).

³M. J. Goldstein, *J. Chem. Phys.* **51**, 3728 (1969).

⁴S. Matsuoka, *Relaxation Phenomena in Polymers* (Hanser, München, 1992), Chap. 2.

⁵O. Yamamuro *et al.*, *J. Phys. Chem. B* **102**, 1605 (1998).

⁶W. Kauzmann, *Chem. Rev.* **43**, 219 (1948).

⁷E. Donth, *J. Non-Cryst. Solids* **53**, 325 (1982).

⁸E. Hempel *et al.*, *J. Phys. Chem. B* **104**, 2460 (2000).

⁹M. Beiner *et al.*, *Europhys. Lett.* **44**, 321 (1998); *Macromolecules* **31**, 8973 (1998).

¹⁰S. Kahle *et al.*, *Macromolecules* **30**, 7214 (1997).

¹¹J. Korus *et al.*, *Acta Polym.* **48**, 369 (1997).

¹²E. Donth (unpublished); E. Donth, E. Hempel, and C. Schick, *J. Phys.: Condens. Matter* **12**, L281 (2000).

¹³M. von Laue, *Phys. Z.* **18**, 542 (1917).

¹⁴E. W. Fischer, E. Donth, and W. Steffen, *Phys. Rev. Lett.* **68**, 2344 (1992).

¹⁵M. L. Williams, R. F. Landel, and J. D. Ferry, *J. Am. Chem. Soc.* **77**, 3701 (1955).

¹⁶U. Tracht *et al.*, *Phys. Rev. Lett.* **81**, 2727 (1998).

¹⁷M. C. Phillips, A. J. Barlow, and J. Lamb, *Proc. R. Soc. London, Ser. A* **329**, 193 (1972).

¹⁸M. Arndt *et al.*, *Phys. Rev. Lett.* **79**, 2077 (1997); E. Hempel *et al.*, *Thermochim. Acta* **337**, 163 (1999).

¹⁹C. Schick and E. Donth, *Phys. Scr.* **43**, 423 (1991).

- ²⁰F. Garwe *et al.*, *Macromolecules* **29**, 247 (1996).
- ²¹A. Arbe, D. Richter, J. Colmenero, and B. Farago, *Phys. Rev. E* **54**, 3853 (1996); E. Donth, K. Schröter, and S. Kahle, *ibid.* **60**, 1099 (1999); A. Arbe *et al.*, *ibid.* **60**, 1103 (1999).
- ²²R. Casalini *et al.*, *Phys. Rev. B* **56**, 3016 (1997).
- ²³E. Hempel, M. Beiner, T. Renner, and E. Donth, *Acta Polym.* **47**, 525 (1996); E. Hempel, S. Kahle, R. Unger, and E. Donth, *Thermochim. Acta* **329**, 97 (1999).
- ²⁴S. S. Chang and A. B. Bestul, *J. Chem. Phys.* **56**, 503 (1972); see also, Ref. 28, p. 143.
- ²⁵R. Richert and C. A. Angell, *J. Chem. Phys.* **108**, 9016 (1998).
- ²⁶A. J. Barlow, J. Lamb, and A. J. Matheson, *Proc. R. Soc. London, Ser. A* **292**, 322 (1966).
- ²⁷W. T. Laughlin and D. R. Uhlmann, *J. Phys. Chem.* **76**, 2317 (1972); M. Cukierman, J. W. Lane, and D. R. Uhlmann, *J. Chem. Phys.* **59**, 3639 (1973).
- ²⁸F. Stickel, Ph.D. thesis, Universität Mainz (Shaker, Aachen, 1995).
- ²⁹F. Stickel, E. W. Fischer, and R. Richert, *J. Chem. Phys.* **104**, 2043 (1996); C. Hansen *et al.*, *ibid.* **107**, 1086 (1997).
- ³⁰E. Donth, *Acta Polym.* **50**, 240 (1999).
- ³¹N. O. Birge and S. R. Nagel, *Phys. Rev. Lett.* **54**, 2674 (1985).
- ³²N. O. Birge, *Phys. Rev. B* **34**, 1631 (1986).
- ³³R. Böhmer, K. L. Ngai, C. A. Angell, and D. J. Plazek, *J. Chem. Phys.* **99**, 4201 (1993).
- ³⁴N. O. Birge and S. R. Nagel, *Rev. Sci. Instrum.* **58**, 1464 (1987).
- ³⁵D. H. Jung *et al.*, *Meas. Sci. Technol.* **3**, 475 (1992).
- ³⁶J. Korus *et al.*, *Thermochim. Acta* **304/305**, 99 (1997).
- ³⁷M. Beiner *et al.*, *Macromolecules* **29**, 5183 (1996).
- ³⁸E. Donth *et al.*, *Macromolecules* **29**, 6589 (1996).
- ³⁹D. J. Plazek, I.-C. Chay, K. L. Ngai, and C. M. Roland, *Macromolecules* **28**, 6432 (1995); D. J. Plazek, *J. Rheol.* **40**, 987 (1996).
- ⁴⁰P. K. Dixon and S. R. Nagel, *Phys. Rev. Lett.* **61**, 341 (1988).
- ⁴¹N. O. Birge, P. K. Dixon, and N. Menon, *Thermochim. Acta* **304/305**, 51 (1997).
- ⁴²N. Menon, *J. Chem. Phys.* **105**, 5246 (1996).
- ⁴³G. P. Johari and M. Goldstein, *J. Chem. Phys.* **53**, 2372 (1970).
- ⁴⁴U. Pschorn *et al.*, *Macromolecules* **24**, 398 (1991).
- ⁴⁵E. Donth, S. Kahle, J. Korus, and M. Beiner, *J. Phys. I* **7**, 581 (1997); S. Kahle, M. Schulz, and E. Donth, *J. Non-Cryst. Solids* **238**, 234 (1998).
- ⁴⁶E. Donth, *Acta Polym.* **30**, 481 (1979).
- ⁴⁷S. Matsuoka, *J. Res. Natl. Inst. Stand. Technol.* **102**, 213 (1997).
- ⁴⁸I. M. Hodge, *J. Res. Natl. Inst. Stand. Technol.* **102**, 195 (1997).
- ⁴⁹S. Reissig, Ph.D. thesis, Universität Halle, 1999; K. Gutewort, Diploma thesis, Universität Halle, 1999.
- ⁵⁰S. Kahle *et al.*, *J. Mol. Struct.* **479**, 149 (1999).
- ⁵¹W. Götze and L. Sjögren, *Rep. Prog. Phys.* **55**, 241 (1992).
- ⁵²S. Kahle, K. Schröter, E. Hempel, and E. Donth, *J. Chem. Phys.* **111**, 6462 (1999).
- ⁵³The senior author (E.D.) profited from a round table discussion on dynamic heterogeneity organized by R. Böhmer at MPI-PMMainz 20 April 1999 with a lively discussion by C.A. Angell, M.D. Ediger, E.W. Fischer, W. Kob, R. Richert, H. Sillescu, H.W. Spiess, and others.
- ⁵⁴W. Feller, *An Introduction to Probability Theory and Its Applications*, 2nd ed. (Wiley, New York, 1971), Vol. II, p. 134.
- ⁵⁵R. Böhmer *et al.*, *J. Non-Cryst. Solids* **235-237**, 1 (1998).
- ⁵⁶S. H. Glarum, *J. Chem. Phys.* **33**, 1371 (1960).
- ⁵⁷G. P. Johari and W. Whalley, *Faraday Symp. Chem. Soc.* **6**, 23 (1972).
- ⁵⁸F. H. Stillinger, *Science* **267**, 1935 (1995).
- ⁵⁹S. Sastry, P. G. Debenedetti, and F. H. Stillinger, *Nature (London)* **393**, 554 (1998).
- ⁶⁰C. A. Angell, *Nature (London)* **393**, 521 (1998).
- ⁶¹E. Donth, *Relaxation and Thermodynamics in Polymers. Glass Transition* (Akademie-Verlag, Berlin, 1992).
- ⁶²J. Brandup and E. H. Immergut, *Polymer Handbook*, 3rd ed. (Wiley, New York, 1989), Chap. V.
- ⁶³J. E. Mark, *Physical Properties of Polymers Handbook* (AIP, Woodbury, New York, 1996), Chaps. 7 and 10.
- ⁶⁴D. W. van Krevelen, *Properties of Polymers. Their Correlation with Chemical Structure; Their Numerical Estimation and Prediction from Additive Group Contributions*, 3rd ed. (Elsevier, Amsterdam, 1990), Part VII.
- ⁶⁵*Landolt-Börnstein, Numerical Data and Functional Relationships in Science and Technology*, edited by K.H. Hellwege, Vol. II/1 (Springer, Berlin, 1971); Vol. IV/4b (1972); Vol. IV/1 (1955).
- ⁶⁶H. F. Mark, N. M. Biklales, C. G. Overberger, and G. Menges, *Encyclopedia of Polymer Science and Engineering*, 2nd ed. (Wiley, New York, 1985), Vols. 2 and 16.
- ⁶⁷For a review of the methods of temperature-modulated calorimetry, see *Proceedings of the IV Lahnwitz-Seminar zur Kalorimetrie* [*Thermochim. Acta* **304/305** (1997)].
- ⁶⁸In principle, any fluctuating pattern of free volume must be reflected by the structure factor $S(Q)$. Its reflection by the Gibbs distribution is not inevitable (Ref. 12) if the thermodynamic description is based on the von Laue approach permitting true temperature fluctuation.